

Queiroz Galvão Atlanta Filed

4D Geomechanical Study for Fault Reactivation, Compaction and Subsidence (Final Report)

Executive Summary

Schlumberger has been commissioned by Queiroz Galvão to conduct a 4-D Geomechanical Study for the Atlanta Field. This report documents the results, which form part of a larger study of the field conducted in several phases. The particular emphasis for this part of the study is on geomechanical effects that might pose a risk to long term well integrity, particularly reservoir compaction and fault reactivation.

The 4D geomechanical model combines stress analysis using the VISAGE™ finite element tool with the dynamic reservoir model that already exists in IMEX.

- The seismic horizons and interpreted faults provided by Queiroz Galvão were incorporated in the construction of the numerical grid.
- The properties were defined based on the 1D MEMs (Mechanical Earth Models) created in another phase of the project for the three offset wells Shel-4, Shel-8 and Shel-19.
- When populating the properties in 3D, the process was guided by the interval velocity cube provided by Queiroz Galvão.
- The pore pressure was provided for two scenarios - with and without active aquifer.
- Two-way coupling was conducted by exchanging in each step the updated porosity and permeability from the Schlumberger side and updated pore pressure from the Queiroz Galvão side.

To allow for uncertainties in some parameters, the study encompassed an extensive sensitivity study. The following cases which were analyzed with specific emphasis on fault reactivation, compaction and subsidence and well as stress and strain calculation.

- Pre-production stress modelling for the base case (the properties taken from the calibrated 1D MEM) was performed to obtain a representative initial stress state prior to production. It was calibrated with the 1D-MEMs.
- Coupled analysis was performed using both 1-way and 2-way methods. The 1-way method passes pressure information from IMEX to VISAGE, but sends nothing back to IMEX. The 2-way method takes pressures from IMEX to VISAGE and returns an updated porosity and permeability to IMEX for the next time-step.
- Two scenarios were considered in IMEX, one with an active aquifer and one without an active aquifer. The latter case gives larger pressure changes and is more critical.
- For two-way coupling time-steps were set in the years 2019, 2024, 2029, 2034, 2039.
- Parametric studies for the fault properties (base and weak faults) for the preproduction state as well as after 30 years of production, for the cases with and without active aquifer.
- Some cases where the intact rock material is purely elastic and some where it can also deform plastically. The faults are always treated as plastic.
- Parametric study for the Poisson's ratio (base, weak and strong values) for the preproduction state as well as after 30 years of production, for the cases with and without active aquifer.
- Presence of a weak top layer (combined with the case of reduced Poisson's ratio and without an active aquifer), which creates the worst case combination of parameters in terms of generating fault reactivation.

The major findings of the study are the following:

- *Production scenarios with and without active aquifer*

The results from the two scenarios differ within the reservoir area. The case of no active aquifer is the more risky one, as the pressures change by larger amounts. In it the stresses are about 13 percent lower than those for the case of an active aquifer. The subsidence and the compaction is 80 percent more for the case of no active aquifer comparison to the case of an active aquifer.
- *Stress calibration*

Preproduction calibration was achieved by setting appropriate boundary conditions on the sides of the model. The required conditions are a gradient for the maximum horizontal stress of about 14.7 kPa/m, and a minimum/maximum stress ratio on the boundary of about 0.99. A good match in stress between VISAGE and the 1D MEM results (which are calibrated to drilling events) was obtained at all three wells.
- *Blind Tests*

The agreement of the 3D results with the 1D MEMs is an encouraging sign that the model will correctly predict stresses throughout the field. To test the influence of each well on final results, three simulations were conducted in which the mechanical property input from each one of the wells (in turn) was removed. The results show how much the stress pattern is dependent on local measurement of properties, and they confirmed that the overall pattern of stress magnitudes and distribution does not vary greatly as the input wells are changed. There can be local effects such as a more compressible area around well 3-Shel 8.

- *Parametric studies on the fault properties*

The fault properties were varied by reducing the normal stiffness by a factor of 10, from a base case of 0.9717 [GPa/m] to 0.09717 [GPa/m]. Similarly, the shear stiffness was reduced from 0.3889 to 0.03889 [GPa/m].

The comparison of the vertical and horizontal stress along the wells shows that the stresses are almost identical despite the change in fault properties. The conclusion is that reduction in the normal and shear stiffness of the faults does not affect the stresses at wells (at the preproduction stage) unless the wells pass very close to or through the faults.

- *Parametric studies on Poisson's ratio*

- Lower Poisson's ratio (not calibrated vs semi-calibrated)*

The lower Poisson's ratio (20 per cent lower than the base case) simulation gives 21 per cent lower stresses in the reservoir area and 5 per cent lower stresses in the seal. It also gives 100 per cent more compaction at the top of the reservoir and at the sea bed. For this case there are significant areas of the fault surfaces that are reactivated.

This is not, however, a simulation that is representative of real conditions, because the stresses obtained are inconsistent with the actual mud weights used during drilling. The simulation is rather an exercise with simple substitution of the new values for the Poisson's ratio. An additional case obtained more representative results, but still without fully calibrating the model. The results of this simulation show higher stresses and no fault reactivation. The conclusion is that even in the case of a low Poisson's ratio, provided a good calibration of the model was done, fault reactivation will not occur.

- Higher Poisson's ratio*

The higher Poisson's ratio (20 per cent higher than the base case, capped at 0.45) simulation gives 1.5 to 2 per cent higher minimum and maximum horizontal stresses relative to the base case, as well as 25 per cent smaller compaction and subsidence. The faults do not reactivate.

- *Elastic vs plastic solutions*

For the preproduction stress state, as well after production of 30 years, the difference between a purely elastic solution for the intact rock and one with plastic deformation is insignificant.

- *Weak layer at the top of the model (near sea bed)*

The to represent the very unconsolidated material at the sea bed, the top layer of the model was made very weak (Young Modulus = 0.1 * base case, UCS = 0.1 * base case, Friction Angle = 0.25 *base case). It is based on some Fugro laboratory data.

The analysis of the results show that the difference between the two cases is mainly restricted to the top layer. For the preproduction state the weak layer case show smaller value for the plastic shear strain as well for the fault slip potential. This difference decreases with depth to become negligible by layer K=11. In the year 2019 the difference between the two models show the same trend, but is smaller.

- *Two-way coupling*

Two-way coupling was conducted by transferring pressure, porosity and permeability files between separate stress and reservoir simulations, but the results should be the same are those that would be obtained if both programs were run in conjunction on the same computer.

The changes in porosity and permeability associated with two-way coupling do affect the pressures in IMEX, with the permeability in some cells changing by up to 30%. The compaction can also be affected on a localized basis, but the interaction between permeability and pressure changes is complex due as the wells can be controlled by production rate or bottom-hole pressure in IMEX.

Analysis of the fault reactivation shows that the differences between the 1-way and 2-way coupled results are negligible:

- Most of the analysis indicates no reactivation risks
- Some reactivation was observed for the case without aquifer, but in isolated areas
- No reactivation risk was observed in the cap rock seal
- When lowering Poisson's ratio, more extensive reactivation results were observed, but this is unrealistic due to the non-calibrated nature of that model.

General conclusions from the whole study are:

- *Concerning validity of the model:* A considerable amount of structural detail is included in the model including reservoir, overburden and underburden horizons, plus faults in the reservoir, overburden and near surface. Mechanical properties are based on a limited number of wells but seem to be fairly consistent across the field. The 3D stress field matches the 1D MEMs, and is likely to be a reasonable guide to stresses in locations where new wells are planned, both for today and for future dates.
- *Concerning compaction:* In most of the cases examined, the compaction at the top of the reservoir is around 0.6m after 10 years and around 1.0m after 30 years. Some cases with low Poisson's ratio give up to 2.0m reservoir compaction after 30 years. The maximum amount of sea bed subsidence tends to be around 75% of the compaction, so 0.75m after 30 years in the base case.

- *Concerning fault reactivation:* In the base case, fault reactivation is restricted to a few cells, whether the criterion for reactivation is based on plastic shear strain or fault slip potential. A wide range of fault and mechanical properties have been used in the modelling to allow for uncertainties, and the most probable scenarios show least reactivation. The one case that does show extensive reactivation is the one with low Poisson's ratio, which has been shown to be unrealistic unless the boundary conditions are re-calibrated (which then eliminates the fault re-activation).
- *Concerning risk of leakage to surface:* Where there is localised fault reactivation, it tends to be restricted to certain depth ranges, such as the top layer (near sea bed) and K=12 in the overburden. Even there, the plastic shear strains tend to be relatively small (below 1%) and the cap rock and other layers tend to be resistant to reactivation. It is therefore considered very unlikely that a pathway for fluids can be created all the way from the reservoir to the sea bed.
- *Concerning future use and development of the model:* Further data acquisition, including log data, core tests and leak-off tests at new wells, would help in constraining the model parameters. For use in history-matching of IMEX and forecasting of future production and well integrity, it would be useful to confirm exactly how IMEX handles porosity updating.

Queiroz Galvão

Atlanta Filed

4D Geomechanical Study for Fault Reactivation, Compaction and Subsidence (Final Report)

II Methodology

This report describes the building of a representative 3D geomechanical model of the Atlanta field, calculation of the pre-production stress state, fault modelling and coupled reservoir geomechanics simulations.

The modelling was done by conducting the following steps:

- Evaluating the existing structural grid of the field given by the IMEX static and dynamic models.
- Embedding the existing structural grid by adding overburden, underburden and sideburdens and creating a bigger one. This procedure is performed for pure numerical reasons, i.e. to avoid localized boundary effects.
- QC for the provided seismic horizons, and correcting them at the places they intersect the reservoir grid.
- Incorporating into the overburden and the underburden the seismic horizons in order to construct the embedded grid.
- Incorporating all sets of faults into the embedded grid.
- Performing a QC of the embedded grid to ensure it is suitable for numerical calculations.
- Using the 1D MEM geomechanical elastic and rock strength properties, for their upscaling along the wells and 3D property population.
- Populating in 3D the rock mechanical properties based on the 1D MEM values and guided by the interval velocity cube.
- The preproduction stress state was calculated by initializing the model to a state of equilibrium after the application of a gravity load and horizontal stress

(see Figure 6). The stresses from the 1D MEM were used for setting the boundary conditions.

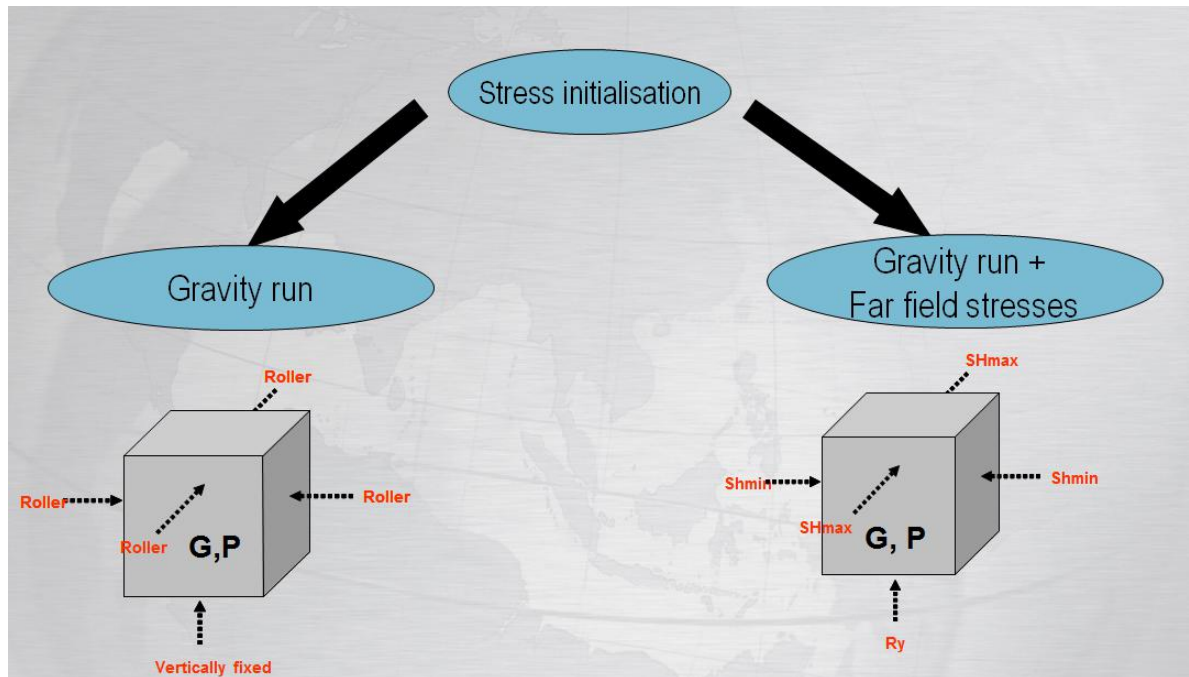


Figure 6: Schema of the 3D numerical model

- Performing different parametric studies regarding the fault properties as well as the Poisson's ratio.
- Performing two-way coupling for the case with and without active aquifer for the years 2019, 2024, 2029, 2034 and 2039. The workflow for the two-way coupling is presented in the figure below

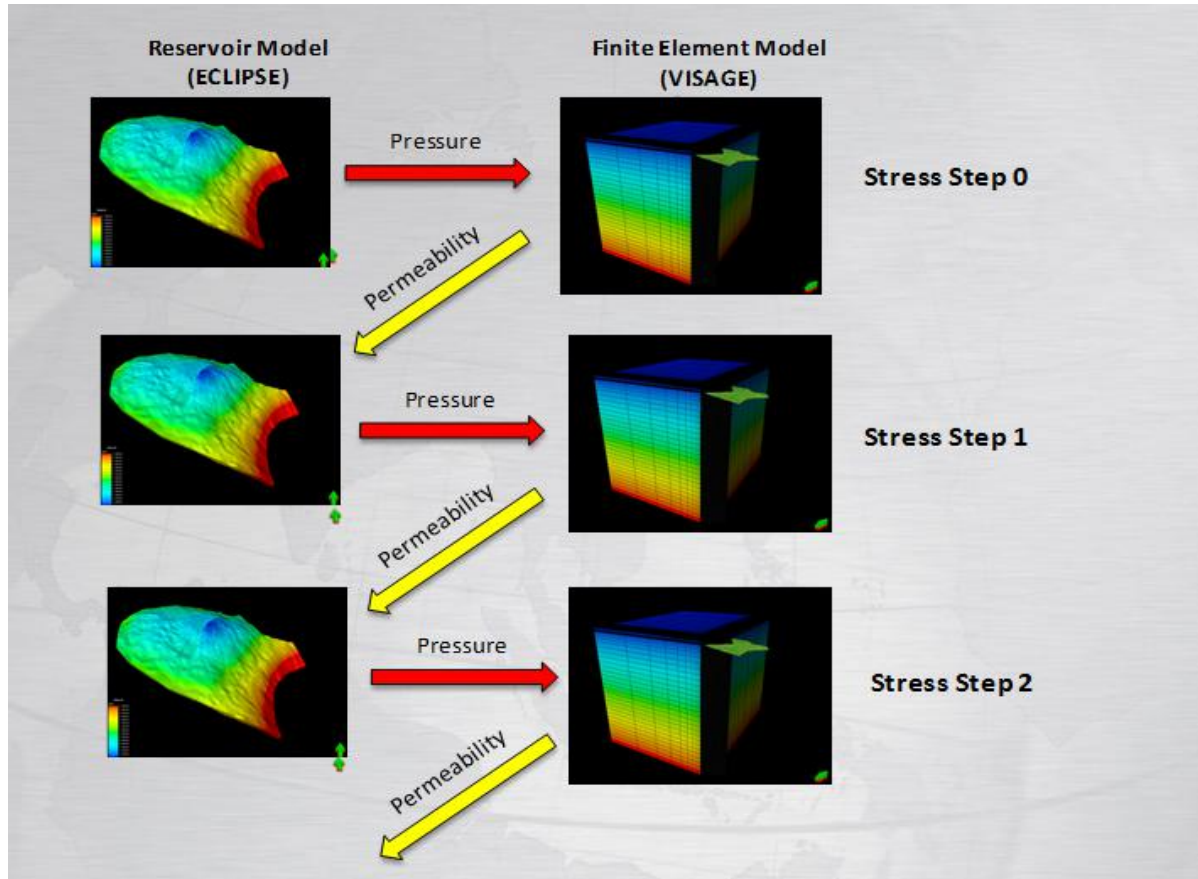


Figure 7: Two-way coupling workflow

II.1 Constitutive Model of Intact Rock

The Mohr-Coulomb elastic-perfectly-plastic constitutive model used for the mechanical modelling of the reservoir, overburden, sideburden and underburden. The total strain tensor $d\bar{\epsilon}$ was the sum of the elastic strain tensor $d\bar{\epsilon}^e$ and the plastic strain tensor $d\bar{\epsilon}^p$:

$$d\bar{\epsilon} = d\bar{\epsilon}^e + d\bar{\epsilon}^p$$

The yield surface was described by a linear function:

$$F = p \sin \phi + J \left(\cos \phi - \frac{\sin \theta \sin \phi}{\sqrt{3}} \right) - c \cos \phi$$

where p is the mean stress, J is the deviatoric stress, c is the cohesion of the material, ϕ is the friction angle and θ is Lode's angle that defines the shape of the yield surface in the deviatoric plane.

The figure below shows the plot of the Mohr-Coulomb failure surface in the system $(-p, J)$:

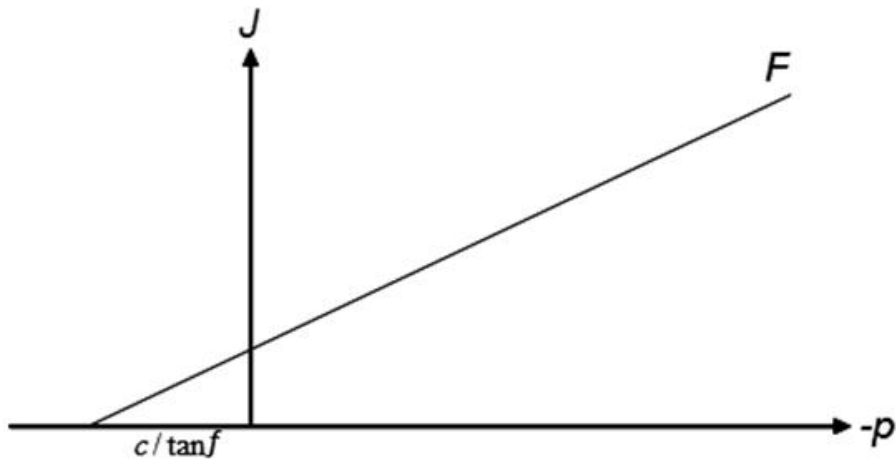


Figure 8: Schematic of the “Mohr-Coulomb” failure surface in p - j space

Experimental results have shown that most geo-materials exhibit a transition from plastic contraction to plastic dilation. It was thus necessary to use a non-associated plastic flow rule. The Mohr-Coulomb plastic potential was defined as:

$$Q = p \sin \psi + J \left(\cos \psi - \frac{\sin \theta \sin \psi}{\sqrt{3}} \right) - c \cos \psi$$

where ψ is the dilation angle that defines the transition zone between plastic contraction and plastic dilation.

II.2 Fault Modelling

The reservoir compaction/heave leads to redistribution of the primary stress-strain field above it. The new field can potentially cause fault slip and thus reactivation. For illustration of this effect we follow the picture of M. Dusseault:

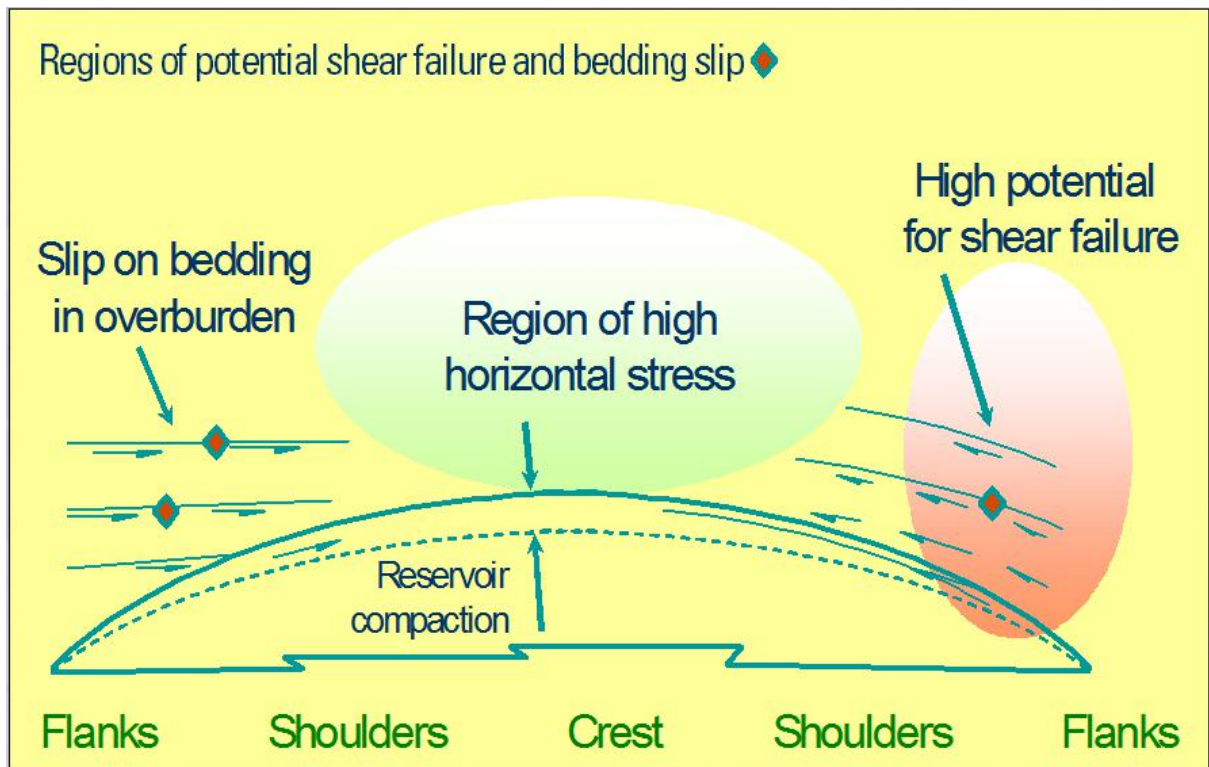


Figure 9: Reservoir compaction effects on the overburden

The fault reactivation phenomenon is very complex and there is no complete physical-mathematical model to generate solutions for all that complexity. Therefore the fault modelling for field evaluation purposes is based on a simplified modelling and heuristical assumptions. Nevertheless, with suitable allowance for uncertainty in the model parameters, there is evidence that the currently available methodology serves reasonably well the needs of the industry.

A) Criteria for fault reactivation:

Schlumberger's methodology has two criteria for fault reactivation.

- **Fault slip potential (SP)** is defined as follows:

$$SP = \frac{\tau(\text{calculated})}{\tau(\text{fault failure})} = \frac{\tau(\text{calculated})}{(\sigma_n \tan \varphi + C)}$$

in which $0 < SP \leq 1$, and where φ is the friction angle of the fault material and C is the cohesion of the fault material. An SP of 1 corresponds to reactivation.

- **Plastic shear strain** on the fault surface bigger than 0.01 (1%) is regarded as significant reactivation.

An illustration of these criteria can be seen in the figure below.

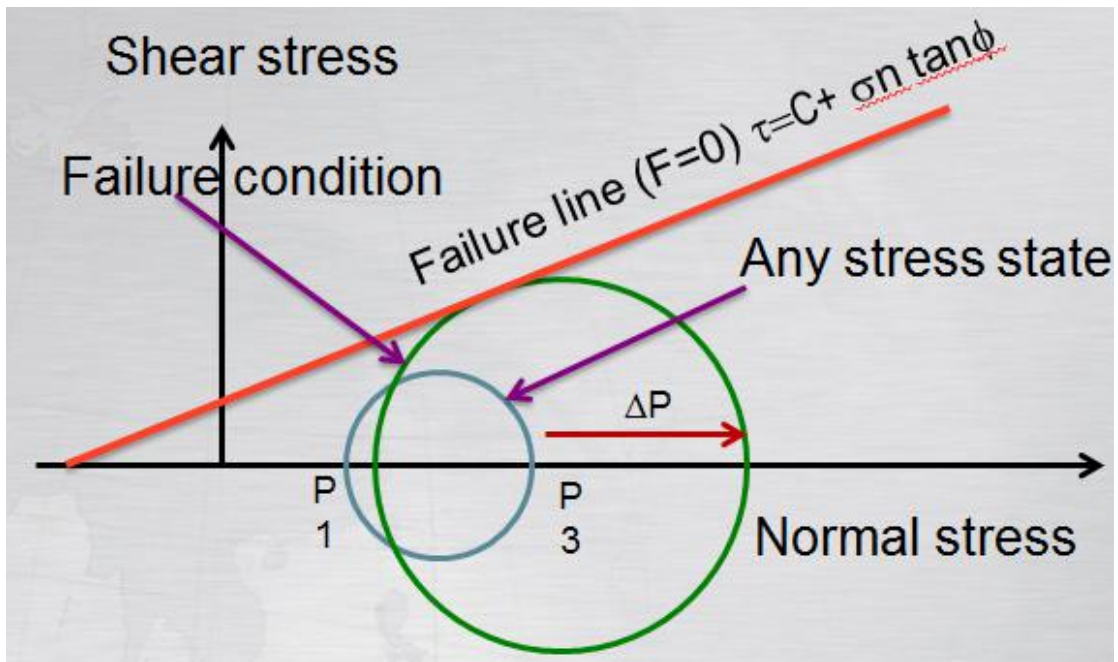


Figure 10: Mohr-Coulomb circle of any stress state and failure line of the fault. Stress states on the failure line have a slip potential of 1

In the picture below, following Byerlee, the stress states are plotted at failure for different rocks.

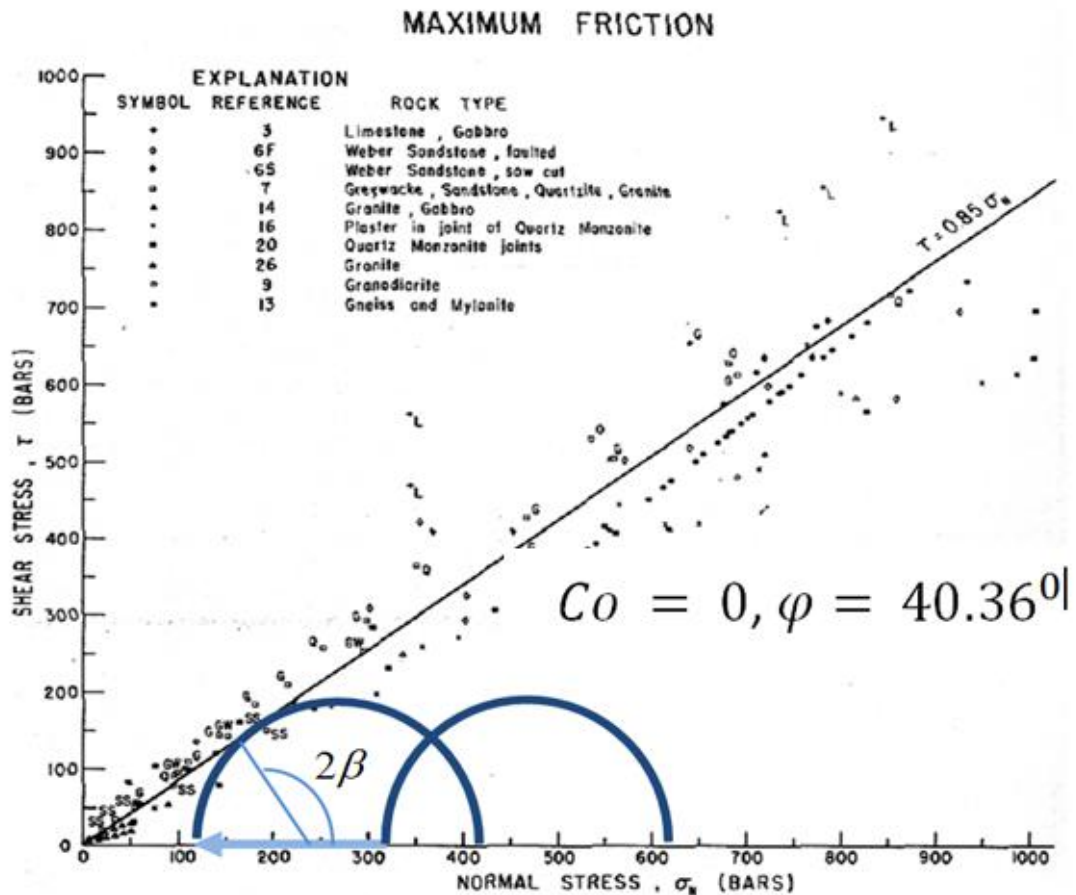


Figure 11: Stress path application over Byerlee's fault criterion

B) Fault modelling in the numerical methods (VISAGE):

In VISAGE, faults and fractures are modelled in a similar way numerically. The method is based on the concept of an equivalent material stiffness, with allowance being made for the orientation of the fractures within each cell.

Consider two sets of fractures A and B . Let the distance between the fractures in the two sets be respectively α and β . Let the normal and shear stiffness of the two fracture sets be respectively (K_n^A, K_s^A) and (K_n^B, K_s^B) . The representative volume (cell) will have a stiffness (elastic) that is a result from the averaging of the intact material stiffness and the stiffness of the fracture sets that intersect that element, as seen in the figure below:

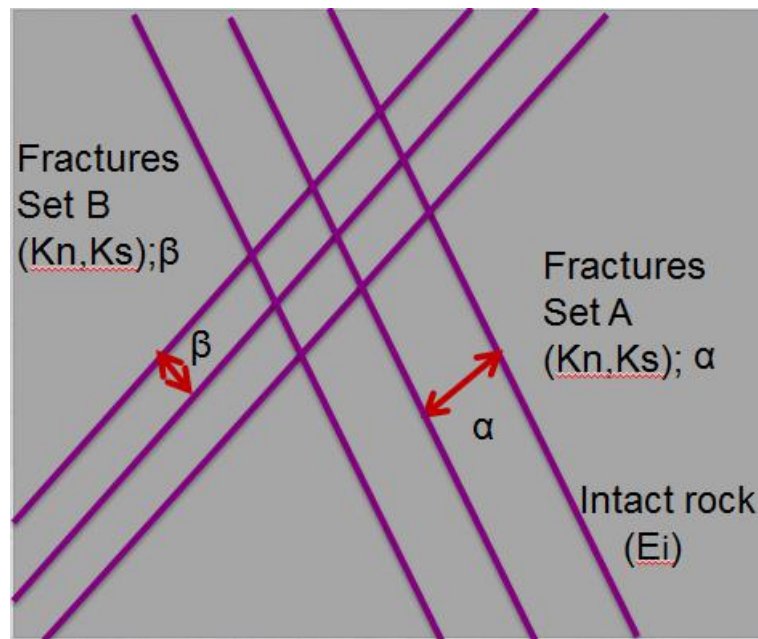


Figure 12: Representative volume element (RVE)

In a similar way we can define equivalent material stiffness for the case of a fault, i.e. when we have one plain of weak material, and where the distance n is defined as the longest normal to the fault plain that intersects the element sides, as seen in the figure below:

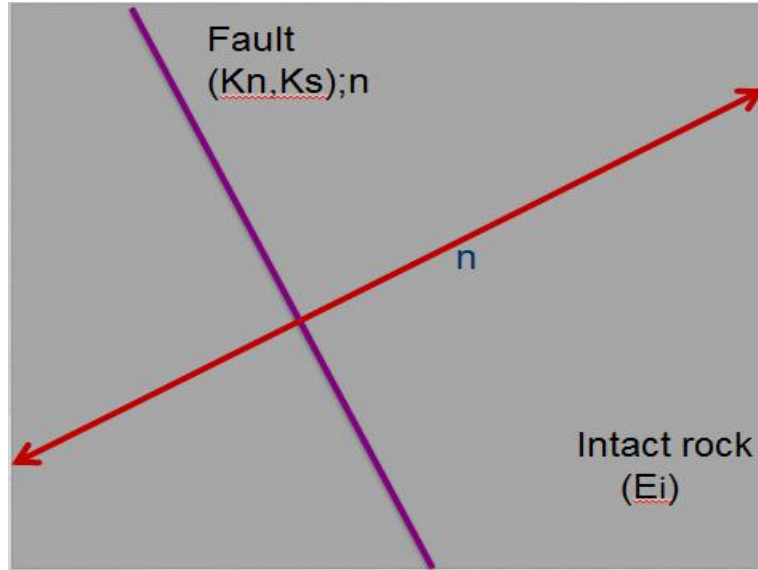


Figure 13: Representative volume element (RVE) for a fault element, where K_n is the normal stiffness of the fault, K_s is the shear stiffness of the fault and E_i is the Young's modulus of the intact rock

The Young's modulus of the equivalent material is the following:

For the 2D case:

$$\frac{1}{E_f} = \frac{1}{E_i} + \frac{1}{nK_n}$$

where E_f is the resulting Young's modulus of the fault element, E_i is the Young's modulus of the intact rock, n is the length of the normal to the fault plane and K_n is the normal stiffness of the fault.

For the 3D case the formula is a bit more complicated and we can derive it as follows:

Consider a joint plane and define local co-ordinate axes (x', y', z') on this plane with z' normal to the plane and x', y' lie within the plane. A compliance matrix s can then be defined which relates stresses on the plane to relative movements:

$$\begin{Bmatrix} w \\ v \\ u \end{Bmatrix} = \begin{bmatrix} S_{11} & S_{12} & S_{13} \\ S_{21} & S_{22} & S_{23} \\ S_{31} & S_{32} & S_{33} \end{bmatrix} \begin{Bmatrix} \sigma_n \\ \tau_{s1} \\ \tau_{s2} \end{Bmatrix}$$

It is unlikely that all 9 components of the compliance matrix will be known. Usually only the normal compliance S_{11} and a general shear compliance S_s will be known. It is assumed that $S_{22} = S_{33}$ the shear compliances are then equal to $S_s\sqrt{2}$ and that all off diagonal terms are zero.

Assuming a set of parallel joints within a set having a joint frequency f and the same compliance on each joint then the overall compliance in the global co-ordinate system is

$$S = fTST^T$$

where T is a transformation matrix from the local joint co-ordinate system to the global system and f is the joint frequency (number of joints per unit length).

If there are n sets of joints, then the total compliance (S^*) is given by

$$S^* = \sum_{i=1}^n f_i T_i S_i T_i^T$$

and the average strain in the joints by

$$\varepsilon_j = S^* \sigma$$

The total strains in the rock mass are the sum of the intact rock strains and the joint strains leading to a final form of the elasticity matrix of the rock mass $[D_{RM}]$ of

$$\sigma = [D_{RM}] \varepsilon$$

$$[D_{RM}] = [[D_I]^{-1} + S^*]^{-1}$$

where $[D_I]$ is the intact rock elasticity matrix. This is the complete form of the elasticity matrix of the “equivalent” material. These equations take into account the elastic characteristics of the joints (through stiffness), the spacing of the joints, orientation of the joints and the elastic characteristics of the intact rock. Formation of the rock mass elasticity as above leads to general anisotropic elasticity matrix.

C) Fault properties:

Fault behaviour depends of a number of parameters such as: friction angle, cohesion, dilatancy, in-situ stresses, and roughness.

Measuring the fault properties can be direct and indirect. The direct measurements can be done when cores from the fault are available. Such cores however are often not available. Even if they are present they reflect the fault property at a discrete location. Thus they may or may not fully represent the overall property of the entire fault as depending on the fault type, their property can vary significantly laterally. There are a few studies that allow to indirectly infer the fault properties. This, however, is a rather new technique, that requires significant amount of a priori information, and is not yet established in the industry.

The general industry practice based on experience and heuristical reasoning uses the following fault properties:

- Friction angle = $0.75 * (\text{Intact rock friction angle})$
- Cohesion = 0 (in case of the conservative approach), or very low values up to about 12 – 14 kPa
- Dilatancy = Friction angle – 30 deg

In the numerical modelling the following properties are used:

- Normal stiffness = Young’s modulus of the surrounding rock/average cell size ($K_n = E/t$)
- Shear stiffness = Normal stiffness/ ~ 2 ($K_s = K_n/\sim 2$)

Schlumberger Geomechanics Center of Excellence based on experience uses the following values for the fault properties:

| Fault Property | Value |
|-------------------------------|---------------------------------------|
| Kn (Normal stiffness) [GPa/m] | 0.5<=5<50 |
| Ks (Shear stiffness) [GPa/m] | 0.25<=2.5<=25 |
| Friction Angle [degree] | 20-35 |
| Dilation angle [degree] | 10 or 1/2 (1/3) of the Friction angle |
| Cohesion [KPa] | 0 |

Table 2: Fault properties used by Schlumberger – Geomechanics Center of Excellence

II.3 Two-Way Coupling

Coupling is a method of linking the VISAGE geomechanical model to the IMEX model that calculates flow and pore pressures in the reservoir. In ‘one-way’ coupling, information (in the form of pore pressures) is only passed from IMEX to VISAGE. The ‘two-way’ designation refers to information being passed in both directions between the simulators: pressures at each time-step are output from IMEX and used as input to VISAGE, while porosity and permeability changes are output from VISAGE and used as input to IMEX.

The porosity update is performed based on the volumetric strain.

The permeability update is, for this study, based on the classical Kozeny-Carman equation:

$$\frac{\Delta p}{L} = \frac{180\bar{V}_0\mu(1-\epsilon)^2}{\Phi_s^2 D_p^2 \epsilon^3}$$

where Δp is the pressure drop, L is the total height of the bed, \bar{V}_0 is the superficial or “empty tower” velocity, μ is the viscosity of the fluid, ϵ is the porosity of the bed, Φ_s is the sphericity of the particles in the packed bed, and D_p is the diameter of the spherical particle.

Ideally, the coupling is performed as part of the same simulation run on a single computer system. Here, however, the VISAGE simulations were performed at the Schlumberger Geomechanics Center of Excellence in Bracknell, UK, while the IMEX simulations were performed at the Queiroz Galvão offices in Rio. This separation of the software does not invalidate the procedure, it simply slows down the interchange while files are transferred.

It has been assumed, for the purposes of this study, that the input of porosity changes in IMEX is being done in a way that suitably preserves fluid mass (e.g. by adjusting

fluid density and pressure when pore volume is reduced). More detailed analysis of the inner workings of IMEX would be required to confirm whether that is the case. The results of the two-way coupling should therefore be regarded as illustrative only, and not relied on for detailed history-matching and forecasting.

